

A finite element method by patch reconstruction for the Stokes problem using mixed formulations

Ruo Li^a, Zhiyuan Sun^b, Fanyi Yang^b, Zhijian Yang^c

^a*CAPT, LMAM and School of Mathematical Sciences, Peking University, Beijing 100871, P. R. China*

^b*School of Mathematical Sciences, Peking University, Beijing 100871, P. R. China*

^c*School of Mathematics and Statistics, Wuhan University*

Abstract

In this paper, we develop a patch reconstruction finite element method for the Stokes problem. The weak formulation of the interior penalty discontinuous Galerkin is employed. The proposed method has a great flexibility in velocity-pressure space pairs whose stability properties are confirmed by the inf-sup tests. Numerical examples show the applicability and efficiency of the proposed method.

Keywords: Stokes problem · Reconstructed basis function · Discontinuous Galerkin method · Inf-sup test

2010 MSC: 49N45, 65N21

1. Introduction

We are concerned in this paper with the incompressible Stokes problem, which has a wide range of applications on the approximation of low Reynolds number flows and the time discretizations of the Oseen equation or Navier-Stokes equation. One of the major difficulties in finite element discretizations for the Stokes problem is the incompressible constraint, which leads to a saddle-point problem. The stability condition often referred as the inf-sup (LBB) condition requires the approximation spaces for velocity and pressure need to

Email addresses: rli@math.pku.edu.cn (Ruo Li), zysun@math.pku.edu.cn (Zhiyuan Sun), yangfanyi@pku.edu.cn (Fanyi Yang), zjyang.math@whu.edu.cn (Zhijian Yang)

be carefully chosen [1]. We refer to [2, 3] for some specific spaces used in the traditional finite element methods to solve the Stokes problem.

Most recently, the discontinuous Galerkin (DG) methods have achieved a great success in computational fluid dynamics, see the state of art survey [4]. Hansbo and Larson propose and analyze an interior penalty DG method for incompressible and nearly incompressible linear elasticity on triangular meshes in [5] where polynomial spaces of degree k and $k - 1$ are employed to approximate velocity and pressure, respectively. In [6] Toselli considers the hp -approximations for the Stokes problem using piecewise polynomial spaces. The uniform divergence stability and error estimates with respect to h and p are proven for this DG formulation when velocity is approximated one or two degrees higher than pressure. Numerical results show that using equal order spaces for velocity and pressure can also work well. Schötzau et al. improve the estimates on tensor product meshes in [7]. A local discontinuous Galerkin method (LDG) for the Stokes problem is proposed in [8]. The LDG method can be considered as a stabilized method when the approximation spaces for velocity and pressure are chosen with the same order. Hybrid discontinuous Galerkin methods are also of interest due to their capability of providing a superconvergent post processing, we refer to [9, 10, 11, 12] for more discussion.

Some special finite element spaces can be adopted to Stokes problem in DG framework. Karakashian and his coworkers [13, 14] propose a DG method with piecewise solenoidal vector fields which are locally divergence-free. Cockburn et al. [15, 16, 9, 17] develop the LDG method with solenoidal vector fields. By introducing the hybrid pressure, the pressure and the globally divergence-free velocity can be obtained by a post-process of the LDG solution. While Montlaur et al. [18] present two DG formulations for the incompressible flow, the first formulation is derived from an interior penalty method such that the computation of the velocity and the pressure is decoupled and the second formulation follows the methodology in [13]. With an inconsistent penalty, the velocity can be computed with absence of pressure terms. Liu [19] presents a penalty-factor-free DG formulation for the Stokes problem with optimal error estimates.

However, one of the limitations of DG methods is the computational cost is higher than using continuous Galerkin method directly [20, 21] because of the duplication of the degrees of freedom at interelement boundaries especially in three-dimensional case. In this paper, we follow the methodology in [22, 23] to apply the patch reconstruction finite element method to the Stokes problem. Piecewise polynomial spaces built by patch reconstruction procedure are taken to approximate velocity and pressure. The new space is a sub-space of the common approximation space used in DG framework, which allows us to employ the interior penalty formulation directly to solve the Stokes problem. As we mentioned before, it is important to verify the inf-sup condition for a mixed formulation to guarantee the stability, which is often severe for a specific discretization [24]. We carry out a series of numerical inf-sup tests proposed in [25, 1] to show this method is numerically stable.

The proposed method provides many merits. First, the DOFs of the system are totally decided by the mesh partition and have no relationship with the interpolation order. Then the method is easy to implement on arbitrary polygonal meshes because of the independence between the process of the construction of the space and the geometry structure of meshes. Third, we emphasize that the spaces to approximate velocity and pressure can be engaged with great flexibility. The results of numerical inf-sup tests exhibit the robustness of our method even in some extreme cases.

The outline of this paper is organized as follows. In Section 2, we briefly introduce the patch reconstruction procedure and the finite element space. Then the scheme of the mixed interior penalty DG method and its error analysis for the Stokes problem are presented in Section 3. In Section 4, we briefly review the inf-sup test and carry out a series of numerical inf-sup tests in several situations to show the proposed method satisfies the inf-sup condition. Finally, two-dimensional numerical examples are presented in Section 5 to illustrate the accuracy and efficiency of the proposed approach, and verify our theoretical results.

2. Reconstruction operator

In this section, we will introduce a reconstruction operator which can be constructed on any polygonal meshes and its corresponding approximation properties.

Let $\Omega \subset \mathbb{R}^d, d = 2, 3$, be a convex polygonal domain with boundary $\partial\Omega$. We denote by \mathcal{T}_h a subdivision that partitions Ω into polygonal elements. And let \mathcal{E}_h be the set of $(d-1)$ -dimensional interfaces (edges) of all elements in \mathcal{T}_h , \mathcal{E}_h^i the set of interior faces and \mathcal{E}_h^b the set of the faces on the domain boundary $\partial\Omega$. We set

$$h = \max_{K \in \mathcal{T}_h} h_K, \quad h_K = \text{diam}(K), \quad h_e = \text{diam}(e),$$

for $\forall K \in \mathcal{T}_h, \forall e \in \mathcal{E}_h$. Further, we assume that the partition \mathcal{T}_h admits the following shape regularity conditions [26, 27]:

- H1** There exists an integer number N independent of h , that any element K admits a sub-decomposition $\widetilde{\mathcal{T}}_{h|K}$ made of at most N triangles.
- H2** $\widetilde{\mathcal{T}}_h$ is a compatible sub-decomposition, that any triangle $T \in \widetilde{\mathcal{T}}_h$ is shape-regular in the sense of Ciarlet-Raviart [28]: there exists a real positive number σ independent of h such that $h_T/\rho_T \leq \sigma$, where ρ_T is the radius of the largest ball inscribed in T .

There many useful properties using for the analysis in finite difference schemes and DG framework can be derived from the above assumptions, such as Agmon inequality and inverse inequality [27, 29, 23]:

- M1** [Agmon inequality] There exists C that depends on N and σ but independent of h_K such that

$$\|v\|_{L^2(\partial K)}^2 \leq C \left(h_K^{-1} \|v\|_{L^2(K)}^2 + h_K \|\nabla v\|_{L^2(K)}^2 \right), \quad \forall v \in H^1(K).$$

- M2** [Inverse inequality] There exists C that depends on N and σ but independent of h_K such that

$$\|\nabla v\|_{L^2(K)} \leq Cm^2/h_K \|v\|_{L^2(K)}, \quad \forall v \in \mathbb{P}_m(K).$$

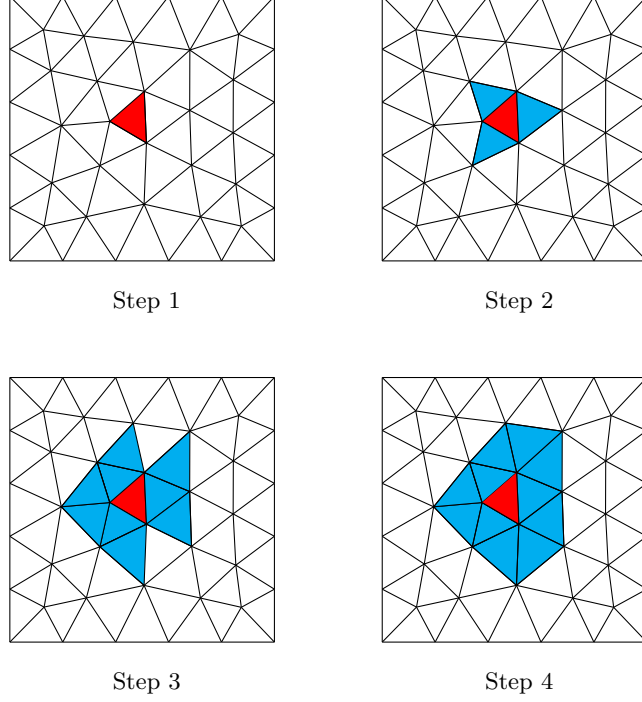


Figure 1: Build patch for $\#S(K) = 12$

Given the partition \mathcal{T}_h , we define the reconstruction operator as follows. First in each element $K \in \mathcal{T}_h$, we specify a point $\mathbf{x}_K \in K$ as the collocation point. Here we just let \mathbf{x}_K be the barycenter of K . Then for each $K \in \mathcal{T}_h$ we construct an element patch $S(K)$, which is a set of K itself and some elements around K . Specifically, we construct $S(K)$ in a recursive manner. For element K , we set $S(K) = \{K\}$ first, and we enlarge $S(K)$ by adding all the von Neumann neighbours (adjacent edge-neighbouring elements) of $S(K)$ into $S(K)$ recursively until we have collected enough elements into the element patch. We denote by $\#S(K)$ the cardinality of $S(K)$ and an example of construction of $S(K)$ with $\#S(K) = 12$ is shown in Fig 1.

For element K , we collect all collocation points in a set \mathcal{I}_K :

$$\mathcal{I}_K \triangleq \left\{ \mathbf{x}_{\tilde{K}} \mid \mathbf{x}_{\tilde{K}} \text{ is the barycenter of } \tilde{K}, \forall \tilde{K} \in S(K) \right\}.$$

Let U_h be the space consisting of piecewise constant functions:

$$U_h \triangleq \{v \in L^2(\Omega) \mid v|_K \in \mathbb{P}_0(K), \forall K \in \mathcal{T}_h\},$$

where \mathbb{P}_n is the polynomial space of degree not greater than n . For any $v \in U_h$, we reconstruct a m th-order polynomial denoted by $\mathcal{R}_K^m v$ on $S(K)$ by the following least squares problem:

$$\mathcal{R}_K^m v = \arg \min_{p \in \mathbb{P}_m(S(K))} \sum_{\mathbf{x} \in \mathcal{I}_K} |v(\mathbf{x}) - p(\mathbf{x})|^2. \quad (2.1)$$

The uniqueness condition for the problem (2.1) is provided by the condition $\#S(K) \geq \dim(\mathbb{P}_m)$ and the following assumption [22, 30]:

Assumption 1. For $\forall K \in \mathcal{T}_h$ and $\forall p \in \mathbb{P}_m(S(K))$, problem (2.1) satisfies

$$p|_{\mathcal{I}(K)} = \mathbf{0} \implies p|_{S(K)} \equiv 0.$$

Hereafter, we assume the uniqueness condition for (2.1) always holds. For any $g \in U_h$, we restrict the definition domain of the polynomial $\mathcal{R}_K^m g$ on element K to define a global reconstruction operator which is denoted by \mathcal{R}^m :

$$\mathcal{R}^m g|_K = (\mathcal{R}_K^m g)|_K, \quad \forall K \in \mathcal{T}_h.$$

Then we extend the reconstruction operator to an operator defined on $C^0(\Omega)$, still denoted as \mathcal{R}^m :

$$\mathcal{R}^m u = \mathcal{R}^m \tilde{u}, \quad \tilde{u} \in U_h, \quad \tilde{u}(\mathbf{x}_K) = u(\mathbf{x}_K), \quad \forall u \in C^0(\Omega).$$

We note that \mathcal{R}^m is a linear operator whose image is actually a piecewise m th-order polynomial space which is denoted as

$$V_h^m = \mathcal{R}^m U_h.$$

Further, we give a group of basis functions of the space V_h^m . We define $w_K(\mathbf{x}) \in C^0(\Omega)$ such that

$$w_K(\mathbf{x}) = \begin{cases} 1, & \mathbf{x} = \mathbf{x}_K, \\ 0, & \mathbf{x} \in \tilde{K}, \quad \tilde{K} \neq K. \end{cases}$$

Then we denote $\{\lambda_K \mid \lambda_K = \mathcal{R}^m w_K\}$ as a group of basis functions. Given λ_K , we may write the reconstruction operator in an explicit way:

$$\mathcal{R}^m g = \sum_{K \in \mathcal{T}_h} g(\mathbf{x}_K) \lambda_K(x), \quad \forall g \in C^0(\Omega). \quad (2.2)$$

From (2.2), it is clear that the degrees of freedom of \mathcal{R}^m are the values of the unknown function at the collocation points of all elements in partition. We present a 2D example in Section 5.1 to demonstrate the reconstruction process and the implementation of basis functions.

We note that $\mathcal{R}^m u (\forall u \in C^0(\Omega))$ may be discontinuous across the inter-element boundaries. The fact inspires us to share some well-developed theories of DG methods and enjoy its advantages.

We first introduce the traditional average and jump notations in DG method. Let e be an interior edge shared by two adjacent elements $e = \partial K^+ \cap \partial K^-$ with the unit outward normal vector \mathbf{n}^+ and \mathbf{n}^- , respectively. Let v and \mathbf{v} be the scalar-valued and vector-valued functions on \mathcal{T}_h , respectively, we define the *average* operator $\{\cdot\}$ as follows:

$$\{v\} = \frac{1}{2}(v^+ + v^-), \quad \{\mathbf{v}\} = \frac{1}{2}(\mathbf{v}^+ + \mathbf{v}^-), \quad \text{on } e \in \mathcal{E}_h^i,$$

with $v^+ = v|_{K^+}$, $v^- = v|_{K^-}$, $\mathbf{v}^+ = \mathbf{v}|_{K^+}$, $\mathbf{v}^- = \mathbf{v}|_{K^-}$.

Further, we set the *jump* operator $[\![\cdot]\!]$ as

$$\begin{aligned} [v] &= v^+ \mathbf{n}^+ + v^- \mathbf{n}^-, \quad [\mathbf{v}] = \mathbf{v}^+ \cdot \mathbf{n}^+ + \mathbf{v}^- \cdot \mathbf{n}^-, \\ [\![\mathbf{v} \otimes \mathbf{n}]\!] &= \mathbf{v}^+ \otimes \mathbf{n}^+ + \mathbf{v}^- \otimes \mathbf{n}^-, \quad \text{on } e \in \mathcal{E}_h^i. \end{aligned}$$

For $e \in \mathcal{E}_h^b$, we set

$$\begin{aligned} \{v\} &= v, \quad \{\mathbf{v}\} = \mathbf{v}, \quad [v] = v\mathbf{n}, \\ [\mathbf{v}] &= \mathbf{v} \cdot \mathbf{n}, \quad [\![\mathbf{v} \otimes \mathbf{n}]\!] = \mathbf{v} \otimes \mathbf{n}, \quad \text{on } e \in \mathcal{E}_h^b. \end{aligned}$$

Now we will present the error analysis of \mathcal{R}^m . We begin by defining broken Sobolev spaces of composite order $\mathbf{s} = \{s_K \geq 0 : \forall K \in \mathcal{T}_h\}$:

$$H^{\mathbf{s}}(\Omega, \mathcal{T}_h) \triangleq \{u \in L^2(\Omega) : u|_K \in H^{s_K}(K), \forall K \in \mathcal{T}_h\},$$

where $H^{s_K}(K)$ is the standard Sobolev spaces on element K . The associated broken norm is defined as

$$\|u\|_{H^s(\Omega, \mathcal{T}_h)}^2 = \sum_{K \in \mathcal{T}_h} \|u\|_{H^{s_K}(K)}^2,$$

where $\|\cdot\|_{H^{s_K}(K)}$ is the standard Sobolev norm on element K . For $\mathbf{u} \in [H^s(\Omega, \mathcal{T}_h)]^d$, the norm is defined as

$$\|\mathbf{u}\|_{H^s(\Omega, \mathcal{T}_h)}^2 = \sum_{i=1}^d \|\mathbf{u}_i\|_{H^s(\Omega, \mathcal{T}_h)}^2.$$

When $s_K = s$ for all elements in \mathcal{T}_h , we simply write $H^s(\Omega, \mathcal{T}_h)$ and $[H^s(\Omega, \mathcal{T}_h)]^d$.

Then we define a constant $\Lambda(m, \mathcal{I}_K)$ for $K \in \mathcal{T}_h$:

$$\Lambda(m, \mathcal{I}_K) \triangleq \max_{p \in \mathbb{P}_m(S(K))} \frac{\max_{\mathbf{x} \in S(K)} |p(\mathbf{x})|}{\max_{\mathbf{x} \in \mathcal{I}_K} |p(\mathbf{x})|}, \quad (2.3)$$

the Assumption 1 is equivalent to

$$\Lambda(m, \mathcal{I}_K) < \infty.$$

The uniform upper bound of $\Lambda(m, \mathcal{I}_K)$ exists if element patches are convex and the triangulation is quasi-uniform [22]. We also refer to [30] for the estimate of $\Lambda(m, \mathcal{I}_K)$ in more general cases such as polygonal partition and non-convex element patch. We denote by Λ_m the uniform upper bound of $\Lambda(m, \mathcal{I}_K)$.

With Λ_m , we have the following estimates.

Lemma 1. *Let $g \in H^{m+1}(\Omega)$ ($m \geq 0$) and $K \in \mathcal{T}_h$, then*

$$\|g - \mathcal{R}^m g\|_{L^2(K)} \lesssim \Lambda_m h^{m+1} \|g\|_{H^{m+1}(S(K))}. \quad (2.4)$$

For convenience, the symbol \lesssim and \gtrsim will be used in this paper. That $X_1 \lesssim Y_1$ and $X_2 \gtrsim Y_2$ mean that $X_1 \leq C_1 Y_1$ and $X_2 \geq C_2 Y_2$ for some positive constants C_1 and C_2 which are independent of mesh size h .

Lemma 2. *Let $g \in H^{m+1}(\Omega)$ ($m \geq 0$) and $K \in \mathcal{T}_h$, then*

$$\|g - \mathcal{R}^m g\|_{L^2(\partial K)} \lesssim \Lambda_m h^{m+\frac{1}{2}} \|g\|_{H^{m+1}(S(K))}. \quad (2.5)$$

For the standard Sobolev norm, we have the following estimates:

Lemma 3. *Let $g \in H^{m+1}(\Omega)$ ($m \geq 0$) and $K \in \mathcal{T}_h$, then*

$$\|g - \mathcal{R}^m g\|_{H^1(K)} \lesssim \Lambda_m h^m \|g\|_{H^{m+1}(S(K))}. \quad (2.6)$$

We refer to [22, 30] for detailed proofs and more discuss about $S(K)$ and $\#S(K)$. Here we note that one of the conditions of guaranteeing the uniform upper bound Λ_m is $\#S(K)$ should be much larger than $\dim(\mathbb{P}_m)$. In Section 4 we will list the values of $\#S(K)$ used in all numerical experiments.

Finally, we derive the estimate in DG energy norm. For the scalar-valued function, the DG energy norm is defined as:

$$\|u\|_{\text{DG}}^2 \triangleq \sum_{K \in \mathcal{T}_h} |u|_{H^1(K)}^2 + \sum_{e \in \mathcal{E}_h} \frac{1}{h_e} \|[[u]]\|_{L^2(e)}^2, \quad \forall u \in H^1(\Omega, \mathcal{T}_h),$$

Theorem 1. *Let $g \in H^{m+1}(\Omega)$ ($m \geq 0$), then*

$$\|g - \mathcal{R}^m g\|_{\text{DG}} \lesssim \Lambda_m h^m \|g\|_{H^{m+1}(\Omega)}. \quad (2.7)$$

Proof. From Lemma 3, we have

$$\begin{aligned} \sum_{K \in \mathcal{T}_h} |g - \mathcal{R}^m g|_{H^1(K)} &\lesssim \sum_{K \in \mathcal{T}_h} \Lambda_m h^m \|g\|_{H^{m+1}(S(K))} \\ &\lesssim \Lambda_m h^m \|g\|_{H^{m+1}(\Omega)}. \end{aligned}$$

For any $e \in \mathcal{E}_h^i$ shared by elements K_1 and K_2 , we have

$$\frac{1}{h_e} \| [g - \mathcal{R}^m g] \|_{L^2(e)}^2 \leq \frac{1}{h_e} \left(\|g - \mathcal{R}^m g\|_{L^2(\partial K_1)}^2 + \|g - \mathcal{R}^m g\|_{L^2(\partial K_2)}^2 \right).$$

From Lemma 2, we get

$$\begin{aligned} \frac{1}{h_e} \|g - \mathcal{R}^m g\|_{L^2(\partial K_1)}^2 &\lesssim \Lambda_m h^{2m} \|g\|_{H^{m+1}(K_1)}^2, \\ \frac{1}{h_e} \|g - \mathcal{R}^m g\|_{L^2(\partial K_2)}^2 &\lesssim \Lambda_m h^{2m} \|g\|_{H^{m+1}(K_2)}^2. \end{aligned}$$

For any $e \in \mathcal{E}_h^b$, assume e is a face of element K , we have

$$\begin{aligned} \frac{1}{h_e} \| [g - \mathcal{R}^m g] \|_{L^2(e)}^2 &\leq \frac{1}{h_e} \| g - \mathcal{R}^m g \|_{L^2(\partial K)}^2 \\ &\lesssim \Lambda_m h^{2m} \| g \|_{H^{m+1}(K)}^2. \end{aligned}$$

Combining the above inequalities gives the estimate (2.7), which completes the proof. \square

For the vector-valued function, the DG energy norm is defined as:

$$\| \mathbf{u} \|_{\text{DG}}^2 \triangleq \sum_{i=1}^d \| \mathbf{u}_i \|_{\text{DG}}^2, \quad \forall \mathbf{u} \in [H^1(\Omega, \mathcal{T}_h)]^d,$$

and the reconstruction operator is defined component-wisely for $[U_h]^d$, still denoted by \mathcal{R}^m :

$$\mathcal{R}^m \mathbf{v} = [\mathcal{R}^m \mathbf{v}_i]^d, \quad 1 \leq i \leq d, \quad \forall \mathbf{v} \in [U_h]^d.$$

Then the operator can be extended on $[C^0(\Omega)]^d$ and the corresponding estimate is written as:

Theorem 2. *let $\mathbf{g} \in [H^{m+1}(\Omega)]^d (m \geq 0)$, then*

$$\| \mathbf{g} - \mathcal{R}^m \mathbf{g} \|_{\text{DG}} \lesssim \Lambda_m h^m \| \mathbf{g} \|_{H^{m+1}(\Omega)}.$$

Proof. It is a direct extension from Theorem 1. \square

3. The weak form of the stokes problem

In this section, we consider the incompressible Stokes problem with Dirichlet boundary condition, which seeks the velocity field \mathbf{u} and its associated pressure p satisfying

$$\begin{aligned} -\Delta \mathbf{u} + \nabla p &= \mathbf{f} && \text{in } \Omega, \\ \nabla \cdot \mathbf{u} &= 0 && \text{in } \Omega, \\ \mathbf{u} &= \mathbf{g} && \text{on } \partial\Omega, \end{aligned} \tag{3.1}$$

where \mathbf{f} is the given source term and \mathbf{g} is a Dirichlet boundary condition that satisfies the compatibility condition

$$\int_{\partial\Omega} \mathbf{g} \cdot \mathbf{n} ds = 0.$$

For positive integer k, k' , we define the following finite element spaces to approximate velocity and pressure:

$$\mathbf{V}_h^k = [V_h^k]^d, \quad Q_h^{k'} = V_h^{k'}.$$

We note that finite element spaces \mathbf{V}_h^k and $Q_h^{k'}$ are the subspace of the common discontinuous Galerkin finite element spaces, which implies that the interior penalty discontinuous Galerkin method [5, 18] can be directly applied to the Stokes problem (3.1).

For a vector \mathbf{u} , we define the second-order tensor $\nabla \mathbf{u}$ by

$$(\nabla \mathbf{u})_{i,j} = \frac{\partial u_i}{\partial x_j}, \quad 1 \leq i, j \leq d.$$

The discrete problem for the Stokes problem (3.1) is as: find $(\mathbf{u}_h, p_h) \in \mathbf{V}_h^k \times Q_h^{k'}$ such that

$$\begin{aligned} a(\mathbf{u}_h, \mathbf{v}_h) + b(\mathbf{v}_h, p_h) &= l(\mathbf{v}_h), \quad \forall \mathbf{v}_h \in \mathbf{V}_h^k, \\ b(\mathbf{u}_h, q_h) &= (q_h, \mathbf{n} \cdot \mathbf{g})_{\partial\Omega}, \quad \forall q_h \in Q_h^{k'}, \end{aligned} \quad (3.2)$$

where symmetric bilinear form $a(\cdot, \cdot)$ is given by

$$\begin{aligned} a(\mathbf{u}, \mathbf{v}) &= \int_{\Omega} \nabla \mathbf{u} : \nabla \mathbf{v} dx \\ &\quad - \int_{\mathcal{E}_h} (\{\nabla \mathbf{u}\} : [\mathbf{v} \otimes \mathbf{n}] + [\mathbf{u} \otimes \mathbf{n}] : \{\nabla \mathbf{v}\}) ds \\ &\quad + \int_{\mathcal{E}_h} \eta [\mathbf{u} \otimes \mathbf{n}] : [\mathbf{v} \otimes \mathbf{n}] ds, \quad \forall \mathbf{u}, \mathbf{v} \in [H^1(\Omega, \mathcal{T}_h)]^d. \end{aligned} \quad (3.3)$$

The term η is referred to as the penalty parameter which is defined on \mathcal{E}_h by

$$\eta|_e = \eta_e, \quad \forall e \in \mathcal{E}_h,$$

and will be specified later. The bilinear form $b(\cdot, \cdot)$ and the linear form $l(\cdot)$ are defined as

$$\begin{aligned} b(\mathbf{v}, p) &= - \int_{\Omega} p \nabla \cdot \mathbf{v} \, dx + \int_{\mathcal{E}_h} \{p\} [\mathbf{v}] \, ds, \\ l(\mathbf{v}) &= \int_{\Omega} \mathbf{f} \cdot \mathbf{v} \, dx - \int_{\mathcal{E}_h^b} \mathbf{g} \cdot (\nabla \mathbf{v} \cdot \mathbf{n}) \, ds + \int_{\mathcal{E}_h^b} \eta \mathbf{g} \cdot \mathbf{v} \, ds, \end{aligned} \quad (3.4)$$

for $\forall \mathbf{v} \in [H^1(\Omega, \mathcal{T}_h)]^d$ and $p \in L^2(\Omega)$.

Now we present the standard continuity and coercivity properties of the bilinear form $a(\cdot, \cdot)$. Actually the bilinear form $a(\cdot, \cdot)$ is a direct extension from the interior penalty bilinear form used for solving the elliptic problems [31]. It is easy to extend the theoretical results of solving the elliptic problems to $a(\cdot, \cdot)$.

Lemma 4. *The bilinear form $a(\cdot, \cdot)$, defined in (3.3), is continuous when $\eta \geq 0$. The following inequality holds:*

$$|a(\mathbf{u}, \mathbf{v})| \lesssim \|\mathbf{u}\|_{\text{DG}} \|\mathbf{v}\|_{\text{DG}}, \quad \forall \mathbf{u}, \mathbf{v} \in [H^1(\Omega, \mathcal{T}_h)]^d.$$

Lemma 5. *Let*

$$\eta|_e = \frac{\mu}{h_e}, \quad \forall e \in \mathcal{E}_h,$$

where μ is a positive constant. With sufficiently large μ , the following inequality holds:

$$|a(\mathbf{u}_h, \mathbf{u}_h)| \gtrsim \|\mathbf{u}_h\|_{\text{DG}}^2, \quad \forall \mathbf{u}_h \in \mathbf{V}_h^k.$$

The detailed proofs of Lemma 4 and Lemma 5 could be found in [32, 5, 18]. We also refer to [32] where a unified method is employed to analyse the choices of the penalty parameter η .

For $b(\cdot, \cdot)$, we have the analogous continuity property.

Lemma 6. *The bilinear form $b(\cdot, \cdot)$, defined in (3.4), is continuous. The following inequality holds:*

$$|b(\mathbf{v}, q)| \lesssim \|\mathbf{v}\|_{\text{DG}} \|q\|_{L^2(\Omega)}, \quad \forall \mathbf{v} \in [H^1(\Omega, \mathcal{T}_h)]^d, \quad \forall q \in L^2(\Omega).$$

Besides the continuity of $a(\cdot, \cdot), b(\cdot, \cdot)$ and the coercivity of $a(\cdot, \cdot)$, the existence of a stable finite element approximation solution (\mathbf{u}_h, p_h) depends on choosing a pair of spaces \mathbf{V}_h^k and $Q_h^{k'}$ such that the following inf-sup condition holds [1] :

$$\inf_{q_h \in Q_h^{k'}} \sup_{\mathbf{v}_h \in \mathbf{V}_h^k} \frac{b(\mathbf{v}_h, q_h)}{\|\mathbf{v}_h\|_{\text{DG}} \|q_h\|_{L^2(\Omega)}} \geq \beta, \quad (3.5)$$

where β is a positive constant.

The finite element space we build depends on the collocation points and element patches, the theoretical verification of the inf-sup condition for the pair $\mathbf{V}_h^k \times Q_h^{k'}$ is very difficult in all situations. Chappelle and Bathe [25] propose a numerical test on whether the inf-sup condition is passed for a given finite element discretization. In next section, we will carry out a series of numerical evaluations for different k and k' to give an indication of the verification of the inf-sup condition.

Then if the inf-sup condition holds, we could state a standard priori error estimate of the mixed method (3.2).

Theorem 3. *Let the exact solution (\mathbf{u}, p) to the Stokes problem (3.1) belong to $[H^{k+1}(\Omega)]^d \times H^{k'+1}(\Omega)$ with $k \geq 1$ and $k' \geq 0$, and let (\mathbf{u}_h, p_h) be the numerical solution to (3.2), and assume that the inf-sup condition (3.5) holds and the penalty parameter η is set properly. Then the following estimate holds:*

$$\|\mathbf{u} - \mathbf{u}_h\|_{\text{DG}} + \|p - p_h\|_{L^2(\Omega)} \lesssim h^s \left(\|\mathbf{u}\|_{H^{k+1}(\Omega)} + \|p\|_{H^{k'+1}(\Omega)} \right), \quad (3.6)$$

where $s = \min(k, k' + 1)$.

Proof. We define $\mathbf{Z}(\mathbf{g}) \subset \mathbf{V}_h^k$ by

$$\mathbf{Z}(\mathbf{g}) = \{\mathbf{v} \in \mathbf{V}_h : b(\mathbf{v}, q) = \int_{\mathcal{E}_h^b} \mathbf{g} \cdot \mathbf{n} q \, ds, \forall q \in Q_h^{k'}\}. \quad (3.7)$$

Consider $\mathbf{w} \in \mathbf{Z}(\mathbf{g})$ and $q \in Q_h^{k'}$. Since Lemma 5, we have

$$\begin{aligned} \|\mathbf{w} - \mathbf{u}_h\|_{\text{DG}}^2 &\lesssim a(\mathbf{w} - \mathbf{u}_h, \mathbf{w} - \mathbf{u}_h) \\ &\lesssim a(\mathbf{w} - \mathbf{u}, \mathbf{w} - \mathbf{u}_h) + a(\mathbf{u} - \mathbf{u}_h, \mathbf{w} - \mathbf{u}_h) \\ &= a(\mathbf{w} - \mathbf{u}, \mathbf{w} - \mathbf{u}_h) - b(\mathbf{w} - \mathbf{u}_h, p - p_h). \end{aligned}$$

Since $\mathbf{w} - \mathbf{u}_h \in \mathbf{Z}(0)$, the q_h can be replaced by any $q \in Q_h^{k'}$, we obtain

$$\|\mathbf{w} - \mathbf{u}_h\|_{\text{DG}}^2 \lesssim a(\mathbf{w} - \mathbf{u}, \mathbf{w} - \mathbf{u}_h) - b(\mathbf{w} - \mathbf{u}_h, p - q).$$

Using Lemma 4 and 6 gives

$$\|\mathbf{u} - \mathbf{u}_h\|_{\text{DG}} \lesssim \|\mathbf{u} - \mathbf{w}\|_{\text{DG}} + \|p - q\|_{L^2(\Omega)}, \quad \mathbf{w} \in \mathbf{Z}(\mathbf{g}), q \in Q_h^{k'}. \quad (3.8)$$

Then we deal with an arbitrary function in \mathbf{V}_h^k . For the fixed $\mathbf{v} \in \mathbf{V}_h^k$, we consider the problem of finding $\mathbf{z}(\mathbf{v}) \in \mathbf{V}_h^k$, such that

$$b(\mathbf{z}(\mathbf{v}), q) = b(\mathbf{u} - \mathbf{u}_h, q), \quad q \in Q_h^{k'}.$$

Thanks to the inf-sup condition (3.5) and [1, Proposition 5.1.1, p.270]. We can find a solution $\mathbf{z} \in \mathbf{V}_h^k$, such that

$$\|\mathbf{z}(\mathbf{v})\|_{\text{DG}} \lesssim \sup_{0 \neq q \in Q_h^{k'}} \frac{b(\mathbf{z}(\mathbf{v}), q)}{\|q\|_{L^2(\Omega)}} = \sup_{0 \neq q \in Q_h^{k'}} \frac{b(\mathbf{u} - \mathbf{u}_h, q)}{\|q\|_{L^2(\Omega)}} \lesssim \|\mathbf{u} - \mathbf{u}_h\|_{\text{DG}}. \quad (3.9)$$

Since

$$b(\mathbf{z}(\mathbf{v}) + \mathbf{v}, q) = b(\mathbf{u}_h, q) = \int_{\mathcal{E}_h^b} \mathbf{g} \cdot \mathbf{n} q \, ds, \quad \forall q \in Q_h^{k'},$$

we have $\mathbf{z}(\mathbf{v}) + \mathbf{v} \in \mathbf{Z}(\mathbf{g})$. Taking $\mathbf{w} = \mathbf{z}(\mathbf{v}) + \mathbf{v}$ in (3.8) yields

$$\|\mathbf{u} - \mathbf{u}_h\|_{\text{DG}} \lesssim \|\mathbf{u} - \mathbf{v}\|_{\text{DG}} + \|\mathbf{z}(\mathbf{v})\|_{\text{DG}} + \|p - q\|_{L^2(\Omega)}. \quad (3.10)$$

together with (3.9),

$$\begin{aligned} \|\mathbf{u} - \mathbf{u}_h\|_{\text{DG}} &\lesssim \inf_{\mathbf{v} \in \mathbf{V}_h^k} \|\mathbf{u} - \mathbf{v}\|_{\text{DG}} + \inf_{q \in Q_h^{k'}} \|p - q\|_{L^2(\Omega)} \\ &\lesssim h^k \|\mathbf{u}\|_{H^{k+1}(\Omega)} + h^{k'+1} \|p\|_{H^{k'+1}(\Omega)}. \end{aligned} \quad (3.11)$$

Next we consider the pressure term, let $q \in Q_h^{k'}$. Using the inf-sup condition in (3.5) we have

$$\begin{aligned} \|q - p_h\|_{L^2(\Omega)} &\lesssim \sup_{0 \neq \mathbf{v} \in \mathbf{V}_h^k} \frac{b(\mathbf{v}, q - p_h)}{\|\mathbf{v}\|_{\text{DG}}} \\ &= \sup_{0 \neq \mathbf{v} \in \mathbf{V}_h^k} \frac{b(\mathbf{v}, q - p) + b(\mathbf{v}, p - p_h)}{\|\mathbf{v}\|_{\text{DG}}} \\ &= \sup_{0 \neq \mathbf{v} \in \mathbf{V}_h^k} \frac{b(\mathbf{v}, q - p) - a(\mathbf{u} - \mathbf{u}_h, \mathbf{v})}{\|\mathbf{v}\|_{\text{DG}}} \\ &\lesssim \|p - q\|_{L^2(\Omega)} + \|\mathbf{u} - \mathbf{u}_h\|_{\text{DG}}. \end{aligned} \quad (3.12)$$

From the triangle inequality and (3.12), we obtain

$$\begin{aligned} \|p - p_h\|_{L^2(\Omega)} &\lesssim \|\mathbf{u} - \mathbf{u}_h\|_{\text{DG}} + \inf_{q \in Q_h^{k'}} \|p - q\|_{L^2(\Omega)} \\ &\lesssim h^k \|\mathbf{u}\|_{H^{k+1}(\Omega)} + h^{k'+1} \|p\|_{H^{k'+1}(\Omega)}, \end{aligned} \quad (3.13)$$

and the proof is concluded by combining (3.11) and (3.13). \square

4. Inf-sup test

In this section, we perform the inf-sup tests with some velocity-pressure finite element space pairs to validate the inf-sup condition numerically. After the discretization, the matrix form of the problem (3.2) is obtained,

$$\begin{bmatrix} A & B^T \\ B & 0 \end{bmatrix} \begin{bmatrix} \mathbf{U} \\ \mathbf{P} \end{bmatrix} = \begin{bmatrix} \mathbf{F} \\ \mathbf{G} \end{bmatrix},$$

where the matrix A and the matrix B associate with the bilinear form $a(\cdot, \cdot)$ and $b(\cdot, \cdot)$, respectively. The vector \mathbf{U}, \mathbf{P} is the solution vector corresponding to \mathbf{u}_h, p_h and \mathbf{F}, \mathbf{G} is the right hand side corresponding to \mathbf{f}, \mathbf{g} .

Then the numerical inf-sup test is based on the following lemma.

Lemma 7. *Let S and T be symmetric matrices of the norms $\|\cdot\|_{\text{DG}}$ in \mathbf{V}_h^k and $\|\cdot\|_{L^2(\Omega)}$ in $Q_h^{k'}$, respectively, and let μ_{\min} be the smallest nonzero eigenvalue defined by the following generalized eigenvalue problem:*

$$B^T S^{-1} B \mathbf{V} = \mu_{\min}^2 T \mathbf{V},$$

then the value of β is simply μ_{\min} .

The proof of this lemma can be found in [1, 33]. In numerical tests, we would consider a sequence of successive refined meshes and monitor μ_{\min} of each mesh. If a sharp decrease of μ_{\min} is observed while the mesh size approaches to zero, we could predict that the pair of approximation spaces violates the inf-sup condition. Otherwise, if μ_{\min} stabilizes as the mesh is refined, we can conclude that the inf-sup test is passed.

The numerical tests are conducted with following settings, let Ω be the unit square domain in two dimension and we consider two groups of quasi-uniform meshes which are generated by the software *gmsh* [34]. The first ones are triangular meshes(see Fig 2) and the second ones consist of triangular and quadrilateral elements(see Fig 3). In both cases, the mesh size h is taken by $h = \frac{1}{n}$, $n = 10, 20, 30, \dots 80$.

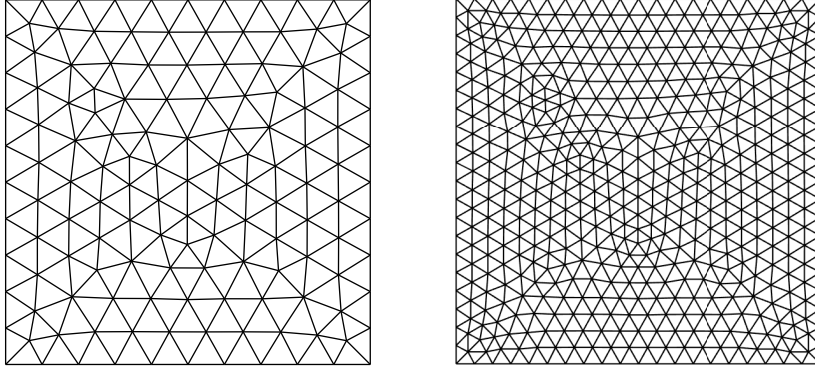


Figure 2: The triangular meshes, $h = \frac{1}{10}$ (left)/ $h = \frac{1}{20}$ (right).

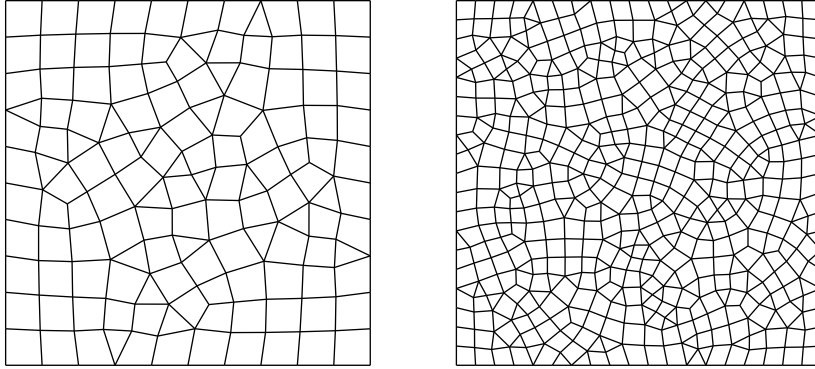


Figure 3: The mixed meshes, $h = \frac{1}{10}$ (left)/ $h = \frac{1}{20}$ (right).

With the given mesh partition, the finite element space can be constructed. As we mention before, for element K , $\#S(K)$ should be large enough to ensure the uniform upper bound Λ_m . For simplicity, $\#S(K)$ is taken uniformly and for different order k we list a group of reference values of $\#S(K)$ for both meshes

in Table 1.

Table 1: choices of $\#S(K)$ for $1 \leq k \leq 5$

order k		1	2	3	4	5
$\#S(K)$	triangular mesh	5	9	18	25	32
	mixed mesh	6	10	20	28	35

We consider three choices of velocity-pressure pairs:

- **Method I.** $(\mathbf{u}_h, p_h) \in \mathbf{V}_h^k \times Q_h^{k-1}$, $1 \leq k \leq 5$.
- **Method II.** $(\mathbf{u}_h, p_h) \in \mathbf{V}_h^k \times Q_h^k$, $1 \leq k \leq 5$.
- **Method III.** $(\mathbf{u}_h, p_h) \in \mathbf{V}_h^k \times Q_h^0$, $1 \leq k \leq 5$.

Here the space Q_h^0 is just the piecewise constant space. These methods correspond to the choices $k' = k$, $k - 1$, 0 , respectively.

Method I. The combination of polynomial degrees for the velocity and pressure approximation spaces is common in traditional FEM and DG while $k \geq 2$, known as Taylor-Hood elements. Numerical results for the method I are shown in Fig 4. μ_{\min} appears to be bounded in every case, which clearly indicates the method I has passed the inf-sup test. It is noticeable that $\mathbf{V}_h^1 \times Q_h^0$ is a stable pair which will lead to the locking-phenomenon in traditional FEM.

Method II. We consider equal polynomial degrees for both approximation spaces. This method is more efficient because the reconstruction procedure is carried out only once. Fig 5 displays the history of μ_{\min} . Similar with method I, the values of μ_{\min} stabilize as h decreases to zero. This method surprisingly keeps valid with $\mathbf{V}_h^1 \times Q_h^1$ which is unstable due to the spurious pressure models in traditional FEM.

Method III. We note that the number of DOFs of our finite element space, which are always equal to the number of elements in partition, has no concern to the order of approximation accuracy. In the sense of that, for all k , high order space V_h^k is in the same size as the piecewise constant piece Q_k^0 . Thus, we take \mathbf{V}_h^k as the velocity approximation space while we select Q_h^0 for the pressure.

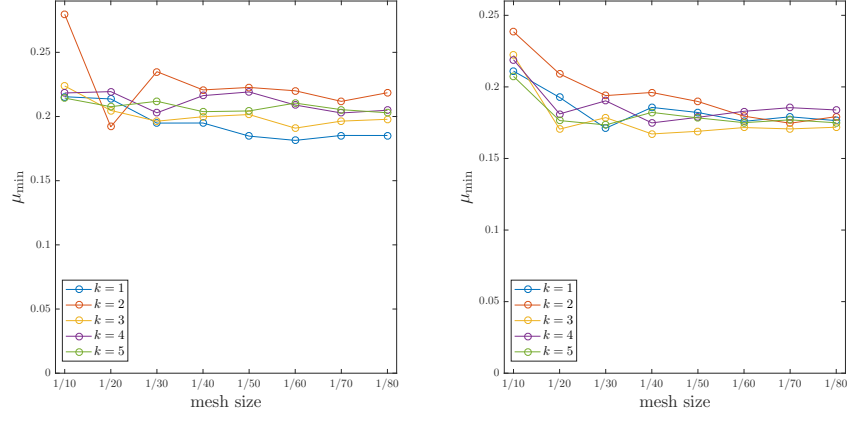


Figure 4: Inf-sup tests for method I on triangular meshes (left) / mixed meshes (right)

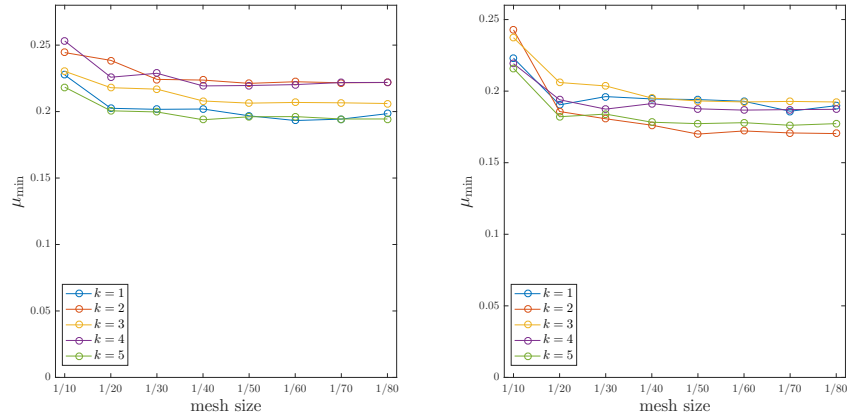


Figure 5: Inf-sup tests for method II on triangular meshes (left) / mixed meshes (right)

Fig 6 summarizes the results of this inf-sup test, which show that the inf-sup condition holds.

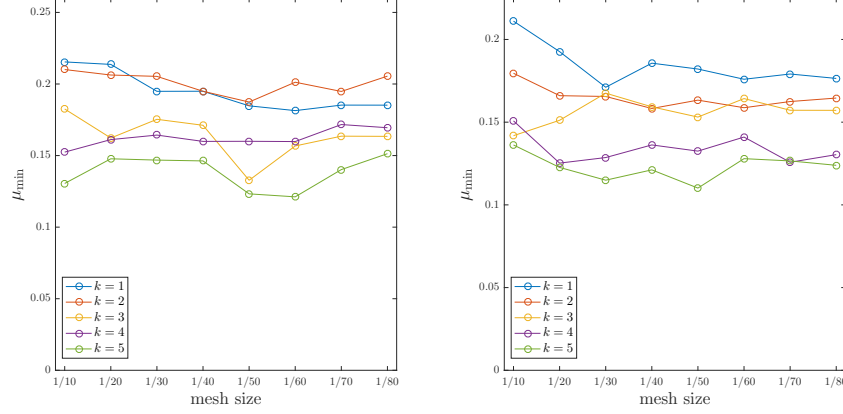


Figure 6: Inf-sup tests for method III on triangular meshes (left) / mixed meshes (right)

The satisfaction of the inf-sup condition has been checked in this section by the numerical tests. All experiments show that the inf-sup value μ_{\min} is bounded. In fact, the combination of two approximation spaces can be more flexible, such as $\mathbf{V}_h^k \times Q_h^{k+1}$ or $\mathbf{V}_h^k \times Q_h^{k+2}$, see Fig 7 and Fig 8. Both cases could pass the inf-sup test. The numerical results demonstrate that our finite element space possesses more robust properties than the traditional finite element method. An analytical proof of the verification of the inf-sup condition is considered as the future work.

5. Numerical Results

In this section, we give some implementation details and some numerical examples in two dimensions to verify the theoretical error estimates in Theorem 3. The numerical settings remain unchanged as in the previous section. For the resulting sparse system, a direct sparse solver is employed to solve it.

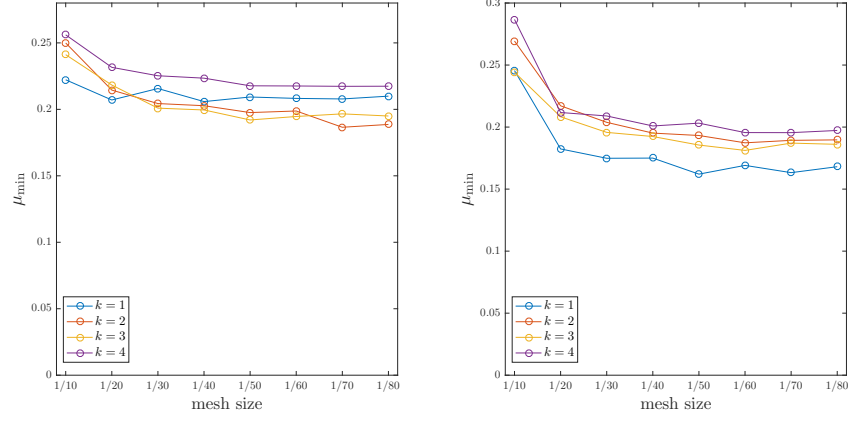


Figure 7: Inf-sup tests for $\mathbf{V}_h^k \times Q_h^{k+1}$ on triangular meshes (left) / mixed meshes (right)

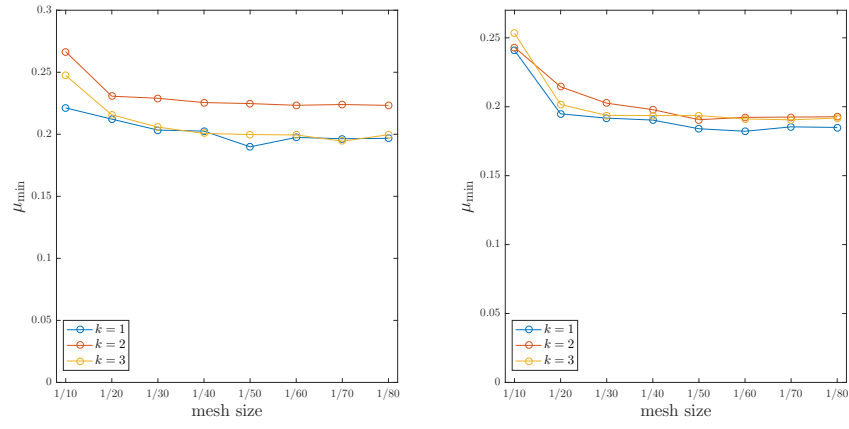


Figure 8: Inf-sup tests for $\mathbf{V}_h^k \times Q_h^{k+2}$ on triangular meshes (left) / mixed meshes (right)

5.1. Implementation

We present a 2D example on the domain $[0, 1] \times [0, 1]$ to illustrate the implementation of our method. The key point is to calculate the basis functions. We consider a quasi-uniform triangular mesh, see Fig 9. Here we consider a

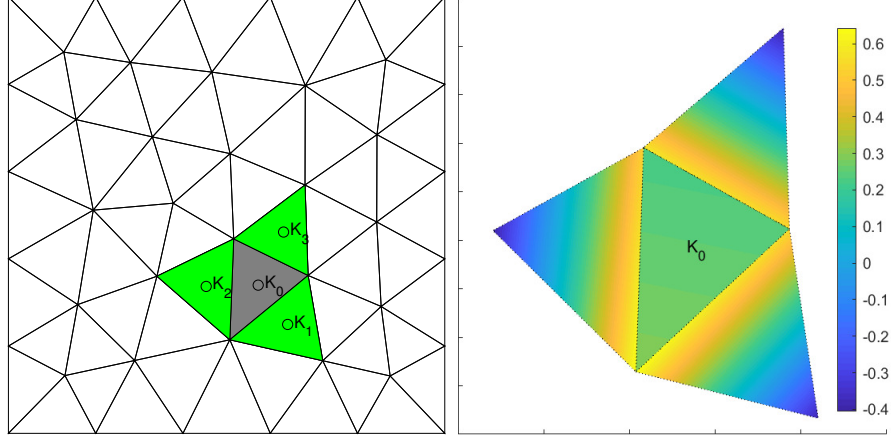


Figure 9: The triangulation and the element patch $S(K_0)$ and the collocation points set \mathcal{I}_{K_0} (left) / the basis function λ_{K_0} (right)

linear reconstruction. The barycenters of all elements are assigned as the collocation points. For any element K , we let $S(K)$ consist of K itself and all edge-neighboring elements. Then we obtain the basis functions by solving the least squares problem on every element.

We take K_0 as an example (see Fig 9), the element patch $S(K_0)$ is chosen as

$$S(K_0) = \{K_0, K_1, K_2, K_3\},$$

and the corresponding collocation points are

$$\mathcal{I}_{K_0} = \{(x_{K_0}, y_{K_0}), (x_{K_1}, y_{K_1}), (x_{K_2}, y_{K_2}), (x_{K_3}, y_{K_3})\},$$

where (x_{K_i}, y_{K_i}) is the barycenter of K_i .

For a continuous function g , the least squares problem is

$$\mathcal{R}_{K_0} = \arg \min_{(a,b,c) \in \mathbb{R}} \sum_{(x_{K'}, y_{K'}) \in \mathcal{I}_{K_0}} |g(x_{K'}, y_{K'}) - (a + bx_{K'} + cy_{K'})|^2.$$

By the Assumption 1, we obtain the unique solution

$$[a, b, c]^T = (A^T A)^{-1} A^T q,$$

where

$$A = \begin{bmatrix} 1 & x_{K_0} & y_{K_0} \\ 1 & x_{K_1} & y_{K_1} \\ 1 & x_{K_2} & y_{K_2} \\ 1 & x_{K_3} & y_{K_3} \end{bmatrix}, \quad q = \begin{bmatrix} g(x_{K_0}, y_{K_0}) \\ g(x_{K_1}, y_{K_1}) \\ g(x_{K_2}, y_{K_2}) \\ g(x_{K_3}, y_{K_3}) \end{bmatrix}.$$

Thus the matrix $(A^T A)^{-1} A^T$ contains all necessary information of the basis functions $\lambda_{K_0}, \lambda_{K_1}, \lambda_{K_2}, \lambda_{K_3}$ on K_0 and we just store it to represent the basis functions. All the basis functions could be obtained by solving the least squares problem on every element. Besides, the basis function λ_{K_0} is presented in Fig 9 and we shall point out that the support of the basis function is not always equal to the element patch, and vice versa.

5.2. 2D smooth problem

We first consider a 2D example on $\Omega = [0, 1]^2$ with smooth analytical solution to investigate the convergence properties. The exact solution is taken as

$$\mathbf{u}(x, y) = \begin{bmatrix} \sin(2\pi x) \cos(2\pi y) \\ -\cos(2\pi x) \sin(2\pi y) \end{bmatrix}, \quad p(x, y) = x^2 + y^2,$$

and the source term \mathbf{f} and the boundary condition \mathbf{g} are chosen accordingly. We consider three methods in Section 4 and solve the Stokes problem on the given triangular meshes and mixed meshes, respectively, with mesh size $h = \frac{1}{n}, n = 10, 20, 40, 80$.

In Fig 10 and Fig 11, we present the L^2 norm and the DG energy norm of the error in the approximation to the exact velocity on both meshes when using method I. And Fig 12 shows the pressure error in L^2 norm. Here we observe that the optimal convergence rates for $\|\mathbf{u} - \mathbf{u}_h\|_{L^2(\Omega)}$, $\|\mathbf{u} - \mathbf{u}_h\|_{\text{DG}}$ and $\|p - p_h\|_{L^2(\Omega)}$ are obtained, which are $O(h^{k+1})$, $O(h^k)$ and $O(h^k)$, respectively. The numerical results confirm the estimate (3.6).

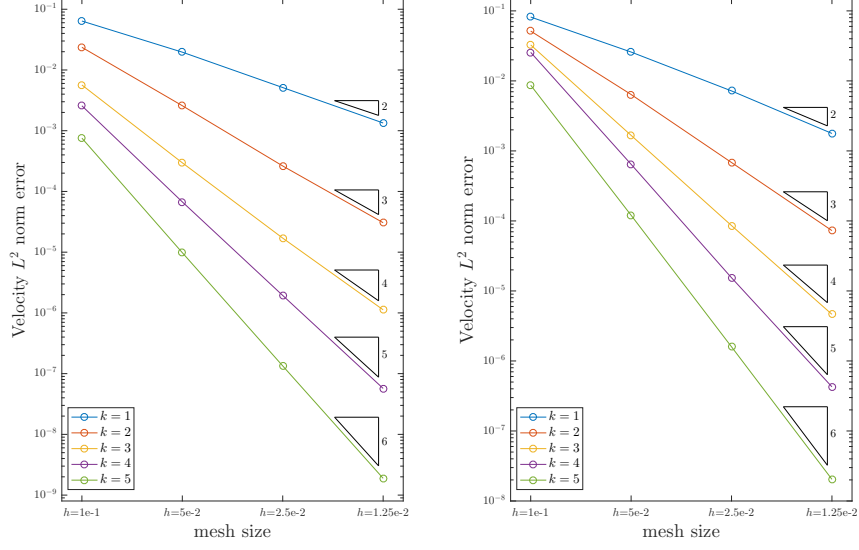


Figure 10: Velocity L^2 norm error with method I for the smooth case on triangular meshes (left) / mixed meshes (right)

Now we consider the method II, the convergence rates are displayed in Fig 13, 14 and 15. All convergence orders are identical to the results in method I, which agrees with the developed theory. For this method, the approximation to the pressure converges in a suboptimal way, but we build the approximation space only once which makes the method II more effective.

Finally, we investigate the numerical performance of the method III. The errors are plotted in Fig 16, 17 and 18. Here the theoretical convergence rates under norm $\|\mathbf{u} - \mathbf{u}_h\|_{\text{DG}}$ and $\|p - p_h\|_{L^2(\Omega)}$ are $O(h^1)$. We observe that the numerical results do not coincide with the theory exactly which results from the numerical error in approximation to pressure is much larger than the interpolation error. The super convergence is spurious and the convergence orders will drop to the expected values as the mesh size h approaches to zero. But it does not imply that the high order is not preferred in method III, the results show that using \mathbf{V}_h^k with larger k could give a more accurate approximation to the

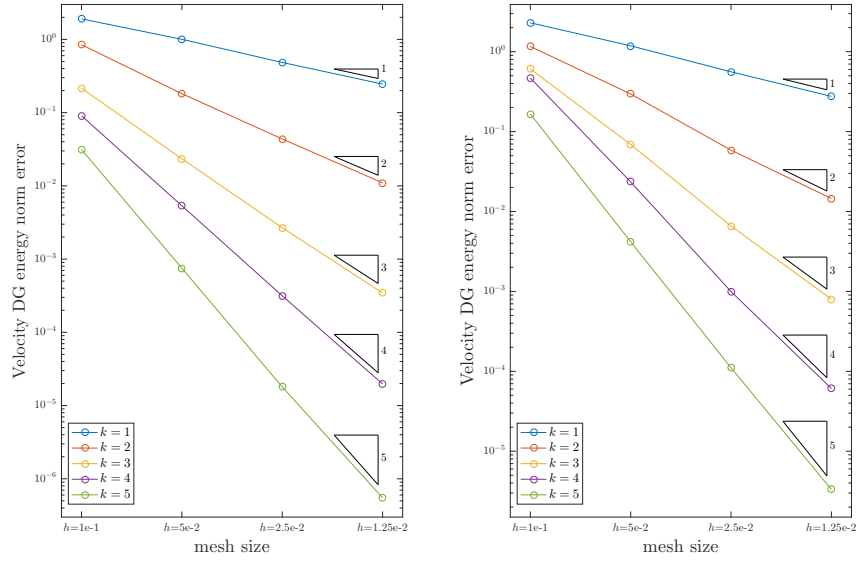


Figure 11: Velocity DG energy norm error with method I for the smooth case on triangular meshes (left) / mixed meshes (right)

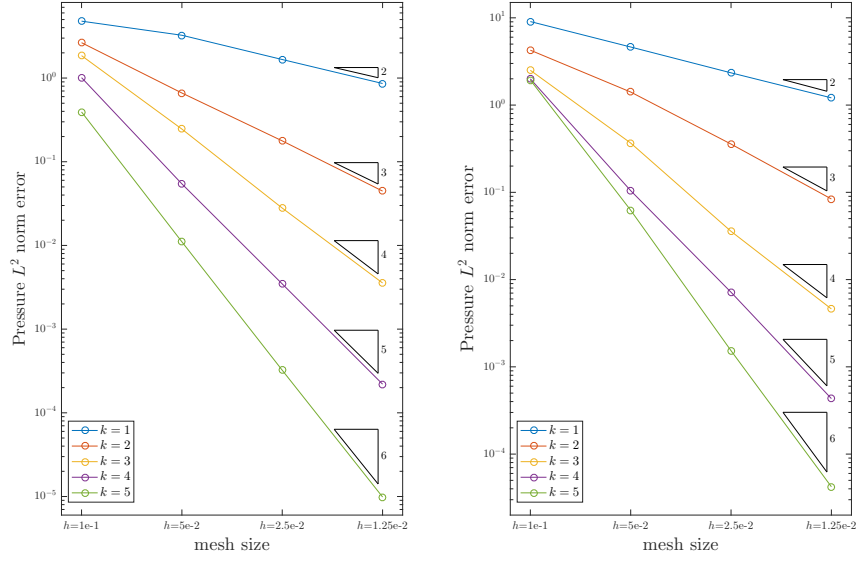


Figure 12: Pressure L^2 norm error with method I for the smooth case on triangular meshes (left) / mixed meshes (right)

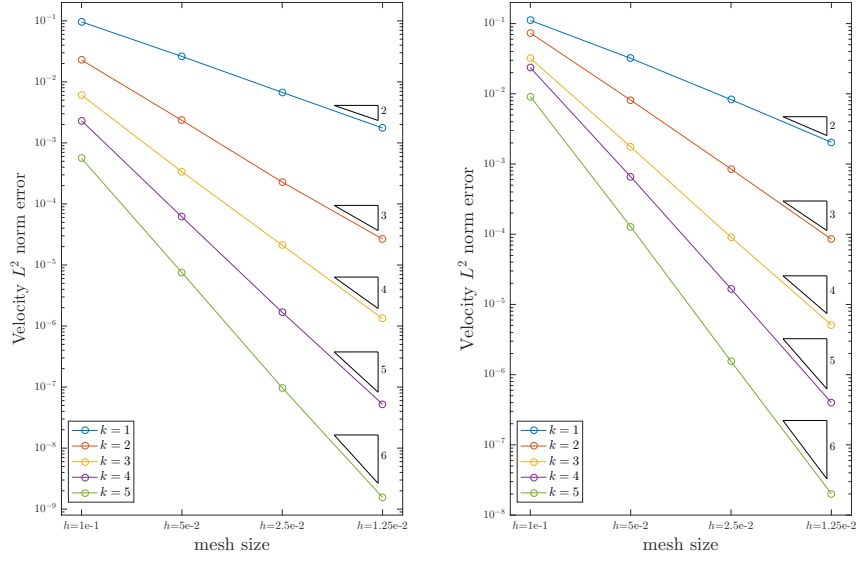


Figure 13: Velocity L^2 norm error with method II for the smooth case on triangular meshes(left) /mixed meshes(right)

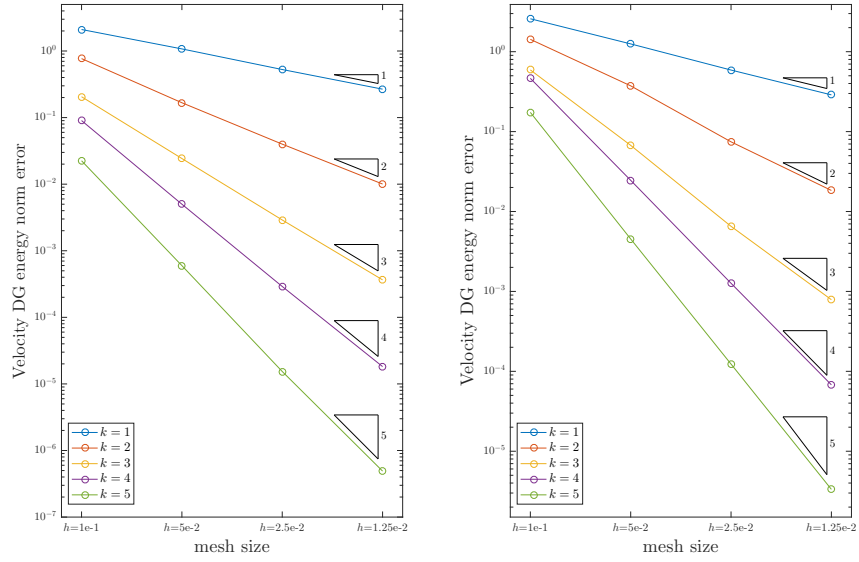


Figure 14: Velocity DG energy norm error with method II for the smooth case on triangular meshes(left)/mixed meshes(right)

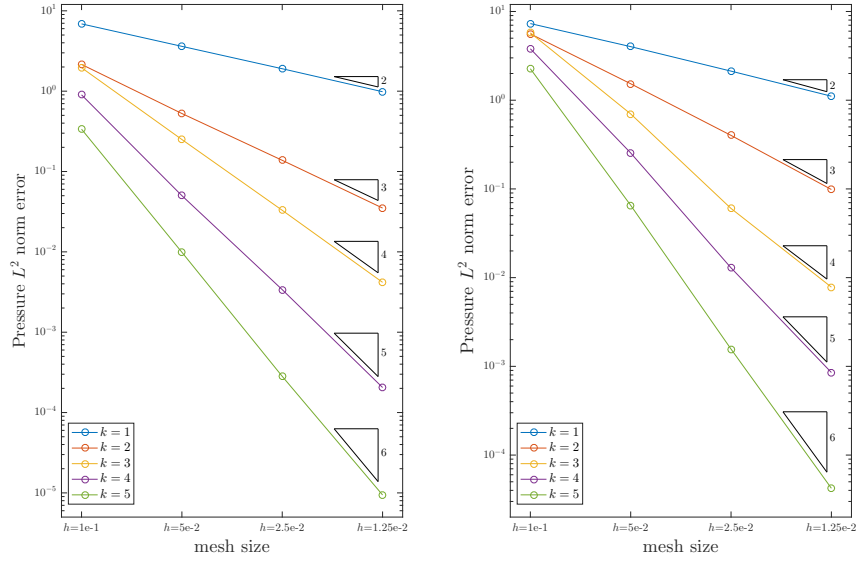


Figure 15: Pressure L^2 norm error with method II for the smooth case on triangular meshes (left)/mixed meshes(right)

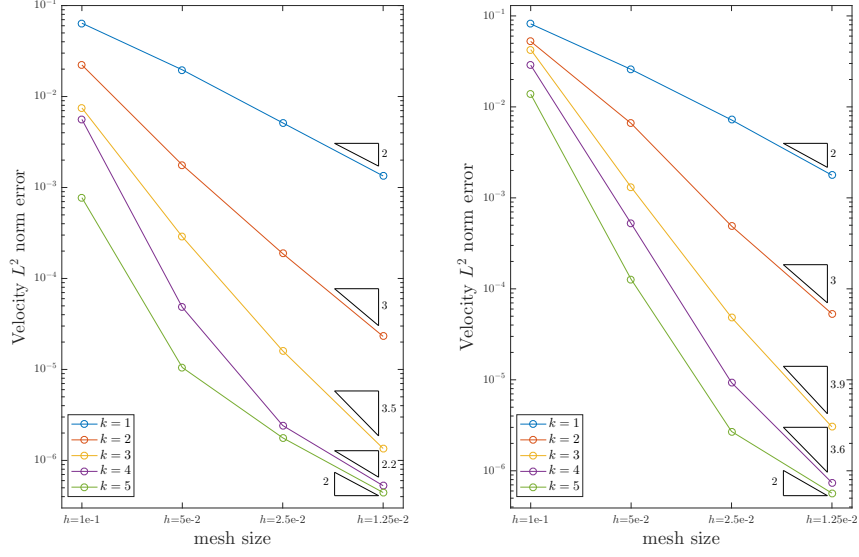


Figure 16: Velocity L^2 norm error on with method III for the smooth case triangular meshes(left)/mixed meshes(right)

velocity and the pressure.

5.3. Driven cavity problem

The driven cavity problem is a standard benchmark test for the incompressible flow. It models a plane flow of an isothermal fluid in a unit square lid-driven cavity. The domain Ω is $[0, 1]^2$ and the boundary condition and the source term are given by

$$\mathbf{g}(x, y) = \begin{cases} (1, 0)^T, & 0 < x < 1, y = 1, \\ (0, 0)^T, & \text{otherwise,} \end{cases} \quad \mathbf{f}(x, y) = \begin{bmatrix} 0 \\ 0 \end{bmatrix}.$$

The domain is partitioned by triangular mesh with mesh size $h = \frac{1}{60}$. Fig 19 shows the velocity vectors and the streamline of the flow for the discretization of $\mathbf{V}_h^3 \times \mathbf{Q}_h^2$. Fig 20 and 21 present the results for the pair of $\mathbf{V}_h^3 \times \mathbf{Q}_h^3$ and $\mathbf{V}_h^3 \times \mathbf{Q}_h^0$, respectively.

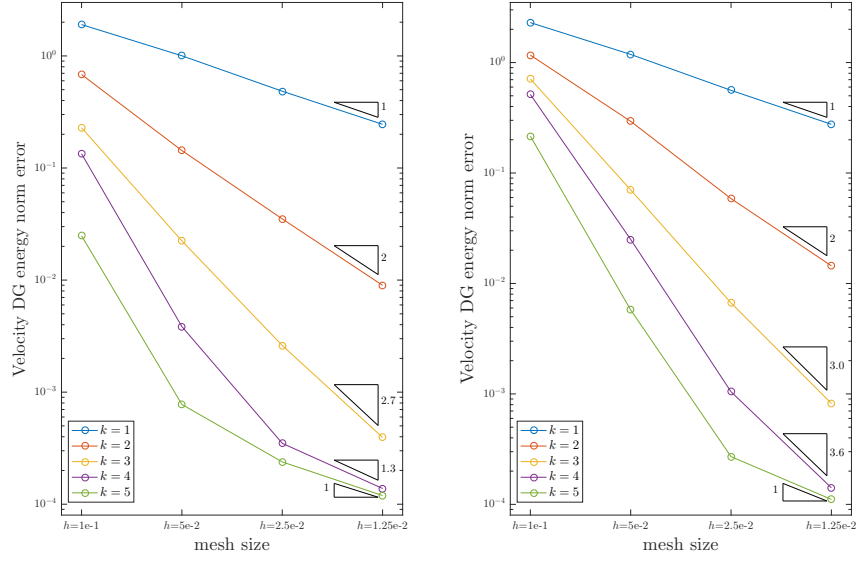


Figure 17: Velocity DG energy norm error with method III for the smooth case on triangular meshes(left)/mixed meshes(right)

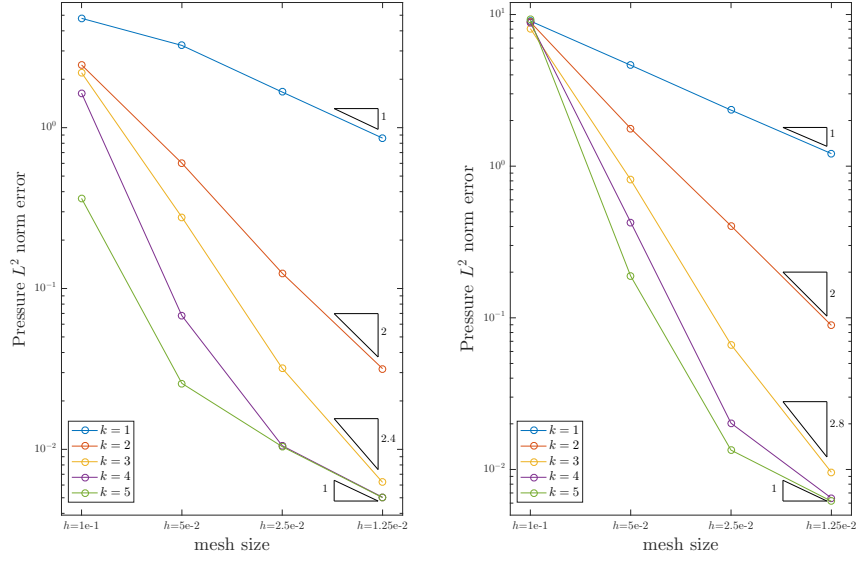


Figure 18: Pressure L^2 norm error on with method III for the smooth case triangular meshes (left)/mixed meshes(right)

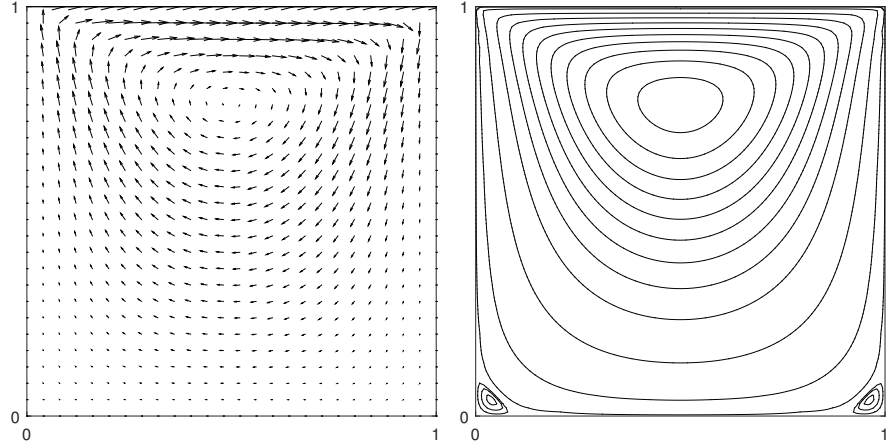


Figure 19: Velocity vectors (left) and the streamline of the flow (right) for $\mathbf{V}_h^3 \times Q_h^2$

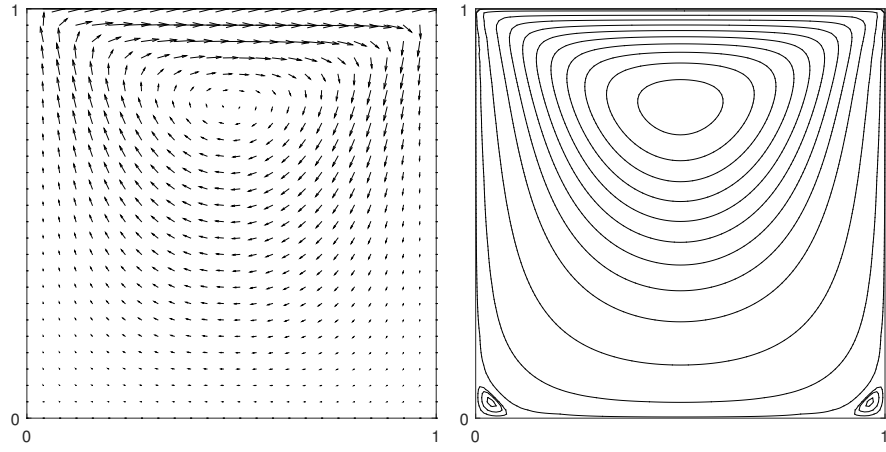


Figure 20: Velocity vectors(left) and the streamline of the flow(right) for $\mathbf{V}_h^3 \times Q_h^3$

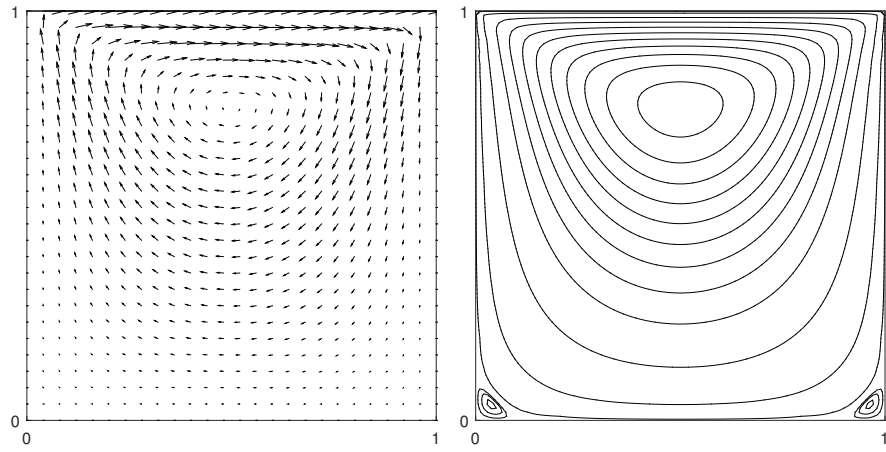


Figure 21: Velocity vectors(left) and the streamline of the flow(right) for $\mathbf{V}_h^3 \times Q_h^0$

5.4. Non-smooth problem

In this example, we investigate the performance of our method dealing with the Stokes problem with a corner singularity in the analytical solution. Let Ω be the L-shaped domain $[-1, 1] \times [-1, 1] \setminus [0, 1] \times (-1, 0]$ and the meshes we use, which are generated by *gmsh*, are refinements of a triangular mesh of 250 triangles (see Fig 22). The exact solution (from [35, 36]) is given by

$$\mathbf{u}(r, \theta) = r^\lambda \begin{bmatrix} (1 + \lambda) \sin(\theta) \psi(\theta) + \cos(\theta) \psi'(\theta) \\ \sin(\theta) \psi'(\theta) - (1 + \lambda) \cos(\theta) \psi(\theta) \end{bmatrix},$$

in polar coordinates, where

$$\begin{aligned} \psi(\theta) = & \frac{1}{1 + \lambda} \sin((1 + \lambda)\theta) \cos(\lambda\omega) - \cos((1 + \lambda)\theta) \\ & - \frac{1}{1 - \lambda} \sin((1 - \lambda)\theta) \cos(\lambda\omega) + \cos((1 - \lambda)\theta), \end{aligned}$$

with $\omega = \frac{3}{2}\pi$ and $\lambda \approx 0.5444837$ as the smallest positive root to

$$\sin(\lambda\omega) + \lambda \sin \omega = 0.$$

At the corner $(0, 0)$, the exact solution contains a singularity which indicates $\mathbf{u}(r, \theta)$ does not belong to $H^2(\Omega)$.

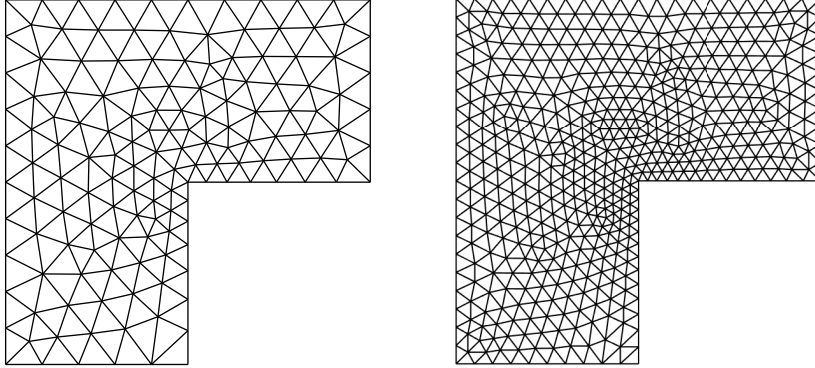


Figure 22: The triangular meshes of L-shaped domain, 250 elements (left)/ 1000 elements (right)

The $\#S(K)$ is chosen also as the Tab 1 shows. In Tab 2 we list the L^2 norm error of the velocity against the degrees of freedom for different pairs

of approximation spaces. We observe that all convergence orders are about 1, which are consistent with the results in [36] where a piece divergence-free discontinuous Galerkin method is developed to solve this problem.

Table 2: Convergence orders of nonsmooth example in L-shaped domain

Method	250 DOFs	1000 DOFs		4000 DOFs		16000 DOFs		64000 DOFs	
	L^2 error	L^2 error	order	L^2 error	order	L^2 error	order	L^2 error	order
$V_h^2 \times Q_h^1$	5.57E-2	2.40E-2	1.21	9.56E-3	1.33	4.61E-3	1.05	2.13E-3	1.10
$V_h^3 \times Q_h^2$	4.97E-2	1.89E-2	1.33	9.29E-3	1.09	4.51E-3	1.04	2.21E-3	1.03
$V_h^2 \times Q_h^2$	4.44E-2	1.58E-2	1.49	7.46E-3	1.08	3.61E-3	1.05	1.73E-3	1.06
$V_h^3 \times Q_h^3$	4.83E-2	1.87E-2	1.37	8.66E-3	1.11	4.11E-3	1.07	1.96E-3	1.07
$V_h^2 \times Q_h^0$	6.59E-2	2.22E-2	1.57	1.03E-2	1.11	5.10E-3	1.01	2.49E-3	1.03
$V_h^3 \times Q_h^0$	6.88E-2	2.71E-2	1.34	9.75E-3	1.47	4.58E-3	1.09	2.18E-3	1.07

6. Conclusion

In this paper, we have introduced a new discontinuous Galerkin method to solve the Stokes problem. A novelty of this method is the new piecewise polynomial space that is reconstructed by solving local least squares problem. A variety of numerical inf-sup tests demonstrate the stability of this method. The optimal error estimates in L^2 norm and DG energy norm are presented and the numerical results are reported to show good agreement with the theoretical predictions.

References

- [1] D. Boffi, F. Brezzi, M. Fortin, [Mixed Finite Element Methods and Applications](#), Vol. 44 of Springer Series in Computational Mathematics, Springer,

Heidelberg, 2013.

URL <https://doi.org/10.1007/978-3-642-36519-5>

- [2] V. Girault, P. A. Raviart, [Finite Element Methods for Navier-Stokes Equations: Theory and Algorithms](#), Springer-Verlag, 1986.

URL <http://dx.doi.org/10.1007/978-3-642-61623-5>

- [3] C. Taylor, P. Hood, [A numerical solution of the Navier-Stokes equations using the finite element technique](#), Internat. J. Comput. & Fluids 1 (1) (1973) 73–100.

URL [https://doi.org/10.1016/0045-7930\(73\)90027-3](https://doi.org/10.1016/0045-7930(73)90027-3)

- [4] B. Cockburn, G. E. Karniadakis, C. W. Shu, [The development of discontinuous Galerkin methods](#), in: Discontinuous Galerkin methods (Newport, RI, 1999), Vol. 11 of Lect. Notes Comput. Sci. Eng., Springer, Berlin, 2000, pp. 3–50.

URL https://doi.org/10.1007/978-3-642-59721-3_1

- [5] P. Hansbo, M. G. Larson, [Discontinuous Galerkin methods for incompressible and nearly incompressible elasticity by Nitsche’s method](#), Comput. Methods Appl. Mech. Engrg. 191 (17-18) (2002) 1895–1908.

URL [https://doi.org/10.1016/S0045-7825\(01\)00358-9](https://doi.org/10.1016/S0045-7825(01)00358-9)

- [6] A. Toselli, [hp discontinuous Galerkin approximations for the Stokes problem](#), Math. Models Methods Appl. Sci. 12 (11) (2002) 1565–1597.

URL <https://doi.org/10.1142/S0218202502002240>

- [7] D. Schötzau, C. Schwab, A. Toselli, [Mixed hp-DGFEM for incompressible flows](#), SIAM J. Numer. Anal. 40 (6) (2002) 2171–2194 (2003).

URL <https://doi.org/10.1137/S0036142901399124>

- [8] B. Cockburn, G. Kanschat, D. Schötzau, C. Schwab, [Local discontinuous Galerkin methods for the Stokes system](#), SIAM J. Numer. Anal. 40 (1) (2002) 319–343.

URL <https://doi.org/10.1137/S0036142900380121>

- [9] J. Carrero, B. Cockburn, D. Schötzau, [Hybridized globally divergence-free LDG methods. I. The Stokes problem](#), Math. Comp. 75 (254) (2006) 533–563.
URL <https://doi.org/10.1090/S0025-5718-05-01804-1>
- [10] P. Lederer, C. Lehrenfeld, J. Schöberl, [Hybrid discontinuous Galerkin methods with relaxed h\(div\)-conformity for incompressible flows. part I](#), SIAM Journal on Numerical Analysis 56 (4) (2018) 2070–2094.
URL <https://doi.org/10.1137/17M1138078>
- [11] N. Nguyen, J. Peraire, B. Cockburn, [A hybridizable discontinuous Galerkin method for stokes flow](#), Computer Methods in Applied Mechanics and Engineering 199 (9) (2010) 582 – 597.
URL <https://doi.org/10.1016/j.cma.2009.10.007>
- [12] B. Cockburn, J. Gopalakrishnan, R. Lazarov, [Unified hybridization of discontinuous galerkin, mixed, and continuous galerkin methods for second order elliptic problems](#), SIAM Journal on Numerical Analysis 47 (2) (2009) 1319–1365.
URL <https://doi.org/10.1137/070706616>
- [13] G. A. Baker, W. N. Jureidini, O. A. Karakashian, [Piecewise solenoidal vector fields and the Stokes problem](#), SIAM J. Numer. Anal. 27 (6) (1990) 1466–1485.
URL <https://doi.org/10.1137/0727085>
- [14] O. A. Karakashian, W. N. Jureidini, [A nonconforming finite element method for the stationary Navier-Stokes equations](#), SIAM J. Numer. Anal. 35 (1) (1998) 93–120.
URL <https://doi.org/10.1137/S0036142996297199>
- [15] B. Cockburn, J. Gopalakrishnan, [Incompressible finite elements via hybridization. I. The Stokes system in two space dimensions](#), SIAM J. Numer. Anal. 43 (4) (2005) 1627–1650.
URL <https://doi.org/10.1137/04061060X>

- [16] B. Cockburn, J. Gopalakrishnan, [Incompressible finite elements via hybridization. II. The Stokes system in three space dimensions](#), SIAM J. Numer. Anal. 43 (4) (2005) 1651–1672.
URL <https://doi.org/10.1137/040610659>
- [17] B. Cockburn, G. Kanschat, D. Schötzau, [A note on discontinuous Galerkin divergence-free solutions of the Navier-Stokes equations](#), J. Sci. Comput. 31 (1-2) (2007) 61–73.
URL <https://doi.org/10.1007/s10915-006-9107-7>
- [18] A. Montlaur, S. Fernandez-Mendez, A. Huerta, [Discontinuous Galerkin methods for the Stokes equations using divergence-free approximations](#), Internat. J. Numer. Methods Fluids 57 (9) (2008) 1071–1092.
URL <https://doi.org/10.1002/fld.1716>
- [19] J. Liu, [Penalty-factor-free discontinuous Galerkin methods for 2-dim Stokes problems](#), SIAM J. Numer. Anal. 49 (5) (2011) 2165–2181.
URL <https://doi.org/10.1137/10079094X>
- [20] O. C. Zienkiewicz, R. L. Taylor, S. J. Sherwin, J. Peiró, [On discontinuous Galerkin methods](#), Internat. J. Numer. Methods Engrg. 58 (8) (2003) 1119–1148.
URL <https://doi.org/10.1002/nme.884>
- [21] A. D. V. D. Montlaur, High-order discontinuous galerkin methods for incompressible flows, Ph.D. thesis, Universitat Politcnica de Catalunya (2009).
- [22] R. Li, P. B. Ming, F. Tang, [An efficient high order heterogeneous multiscale method for elliptic problems](#), Multiscale Model. Simul. 10 (1) (2012) 259–283.
URL <https://doi.org/10.1137/110836626>
- [23] R. Li, P. Ming, Z. Sun, Z. Yang, An Arbitrary-Order Discontinuous

- Galerkin Method with One Unknown Per Element, ArXiv e-prints [arXiv:1803.00378](#).
- [24] K.-J. Bathe, A. Iosilevich, D. Chapelle, [An inf-sup test for shell finite elements](#), Computers & Structures 75 (5) (2000) 439–456.
URL [http://dx.doi.org/10.1016/S0045-7949\(99\)00213-8](http://dx.doi.org/10.1016/S0045-7949(99)00213-8)
 - [25] D. Chapelle, K.-J. Bathe, [The inf-sup test](#), Comput. & Structures 47 (4-5) (1993) 537–545.
URL [https://doi.org/10.1016/0045-7949\(93\)90340-J](https://doi.org/10.1016/0045-7949(93)90340-J)
 - [26] F. Brezzi, A. Buffa, K. Lipnikov, [Mimetic finite differences for elliptic problems](#), ESAIM Numer. Anal. 43 (2009) 277–295.
URL <http://dx.doi.org/10.1051/m2an:2008046>
 - [27] L. Beirão da Veiga, K. Lipnikov, G. Manzini, [The Mimetic Finite Difference Method for Elliptic Problems](#), Vol. 11 of MS&A. Modeling, Simulation and Applications, Springer, Cham, 2014.
URL <https://doi.org/10.1007/978-3-319-02663-3>
 - [28] P. G. Ciarlet, [The Finite Element Method for Elliptic Problems](#), North-Holland, Amsterdam, 1978.
URL <http://dx.doi.org/10.1115/1.3424474>
 - [29] P. F. Antonietti, S. Giani, P. Houston, [hp-version composite discontinuous Galerkin methods for elliptic problems on complicated domains](#), SIAM J. Sci. Comput. 35 (3) (2013) A1417–A1439.
URL <https://doi.org/10.1137/120877246>
 - [30] R. Li, P. B. Ming, Z. Y. Sun, Z. J. Yang, [An arbitrary-order discontinuous Galerkin method with one unknown per element](#), arXiv:1803.00378 [arXiv:1803.00378](#).
URL <http://adsabs.harvard.edu/abs/2018arXiv180300378L>

- [31] D. N. Arnold, [An interior penalty finite element method with discontinuous elements](#), SIAM J. Numer. Anal. 19 (4) (1982) 742–760.
URL <https://doi.org/10.1137/0719052>
- [32] D. N. Arnold, F. Brezzi, B. Cockburn, L. D. Marini, [Unified analysis of discontinuous Galerkin methods for elliptic problems](#), SIAM J. Numer. Anal. 39 (5) (2001/02) 1749–1779.
URL <https://doi.org/10.1137/S0036142901384162>
- [33] D. S. Malkus, [Eigenproblems associated with the discrete LBB condition for incompressible finite elements](#), Internat. J. Engrg. Sci. 19 (10) (1981) 1299–1310.
URL [https://doi.org/10.1016/0020-7225\(81\)90013-6](https://doi.org/10.1016/0020-7225(81)90013-6)
- [34] C. Geuzaine, J. F. Remacle, [Gmsh: A 3-D finite element mesh generator with built-in pre- and post-processing facilities](#), Internat. J. Numer. Methods Engrg. 79 (11) (2009) 1309–1331.
URL <https://doi.org/10.1002/nme.2579>
- [35] R. Verfürth, A Review of A Posteriori Error Estimation and Adaptive Mesh-Refinement Techniques, Wiley-Teubner, 1996.
- [36] P. Hansbo, M. G. Larson, [Piecewise divergence-free discontinuous Galerkin methods for Stokes flow](#), Comm. Numer. Methods Engrg. 24 (5) (2008) 355–366.
URL <https://doi.org/10.1002/cnm.975>